SAR Image Change Detection using Frequency Domain Analysis and Logistic Regression

Course Project as a part of Image and Video Processing Course (EC348)

Submitted by

Adithya Jayan 181EC102
Sujan Amin 181EC247
Venkatvasan R 181EE253

Under the guidance of
Dr. Shyam Lal
in partial fulfilment of the requirements for the award of the degree of
BACHELOR OF TECHNOLOGY

DEPARTMENT OF ELECTRONICS AND COMMUNICATION ENGINEERING
NATIONAL INSTITUTE OF TECHNOLOGY KARNATAKA
SURATHKAL, MANGALORE - 575025

Contents

1 Abstract

Change detection in Multi-temporal Synthetic Aperture Radar(SAR) images is a subject that has various applications. Thus, efficient methods are essential to detect changes in SAR images. The main barrier that arises is speckle noise. This paper discusses a method for change detection in multi-temporal SAR images using frequency domain-based salience detection and logistic regression classification. Its efficiency has been evaluated on multiple datasets and have been compared.

2 Introduction

Synthetic aperture radar (SAR) sensors are a commonly used observation method for land coverage and space-based observation systems. They have various applications such as development monitoring, disaster and flood detection, and land cover estimation and monitoring, among many others.

Since SAR images are pretty resistant to atmospheric distortion and effects of sunlight /illumination, it is ideal for various observation tasks. In particular, multi-temporal SAR images have a wide variety of uses, and thus, difference detection between SAR images is a critical topic of research. Unlike other imaging techniques, due to the high cost of obtaining data and the low amount of existing data available, training a deep learning model is impossible. Thus other methods have to be adopted for the same.

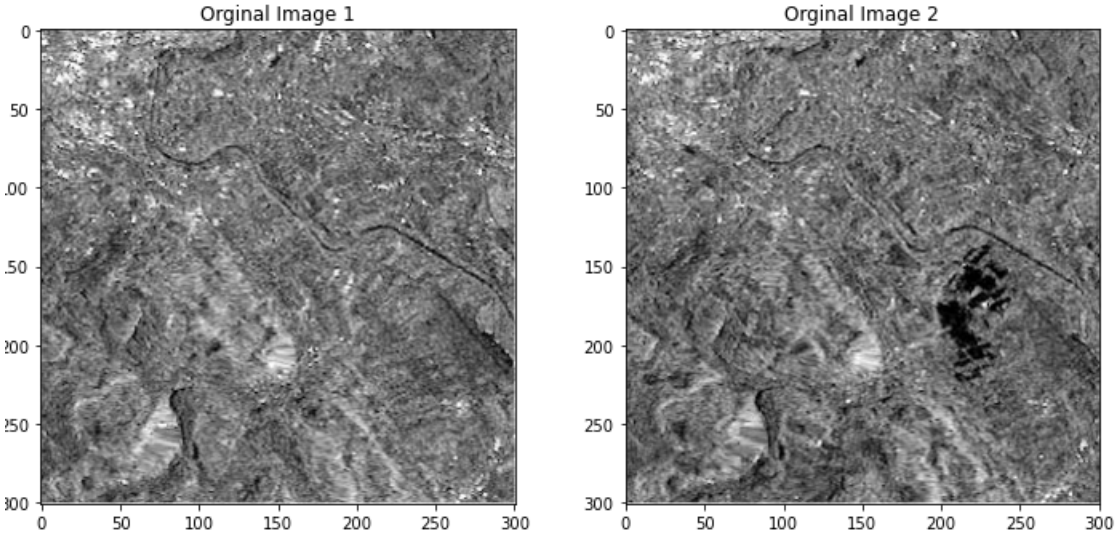

Figure 1: Multi Temporal SAR images from the Bern Dataset

3 Literature Survey

Many methods have been proposed for SAR change detection. In [2] , extreme learning machines combined with Neighbor hood-based ratios were used to obtain the difference. [5] used Gabor feature-based unsupervised change detection. [1] made use of principal component analysis (PCA) to obtain eigenvectors and k-means clustering to classify and obtain the difference image. Fuzzy clustering with a modified MRF energy function for SAR change detection has been presented in [4]. All these methods have shown good results in obtaining difference images.

[3] made use of Frequency-domain analysis and random multi-graph based classification for change detection and has also shown promising results. We have attempted to implement a modified version of this paper below by using frequency domain analysis for obtaining salient regions followed by k-means clustering and Logistic regression for extracting the difference image.

4 Methodology

Log difference is an efficient way to calculate the difference image of the multi temporal SAR images as it converts the multiplicative speckle noise present in SAR images into additive noise. After this, salience detection using frequency domain analysis is done to obtain the most salient regions. These are used to obtain change candidates. The change candidates are then segmented into changed, unchanged and tentative regions using k-means clustering.

Patches are extracted from both the temporally different images and joined to get a features that are a good representation of each pixel and its context. This data is combined with the changed and unchanged labels from the segmentation step and is used as train data. The pixel features belonging to the third segment will be the test data that the classifier will predict for fine-detail segmentation. The changed and unchanged regions are then used to train a Logistic regression classifier. This classifier is used to classify the tentative segment into changed and unchanged regions to obtain the final binary difference image.

4.1 Difference Image generation

The difference image is generated by subtracting the two images pixel-by-pixel using the log operator.

$$I_D = |log(I_1) - log(I_2)| \tag{1}$$

where I_D is the difference image, I_1 and I_2 are the input images

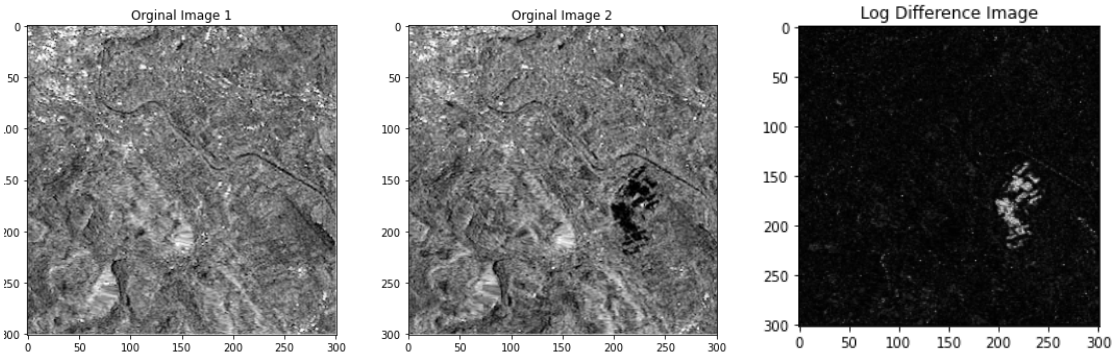

Figure 2: Log Difference Image

4.2 Coarse Changed Region Localization based on Frequency-Domain Analysis

Changed regions are bright regions that are quite distinctive compared to the other regions of the image, as these regions attract greater attention from the human visual system. Frequency domain-based salience detection[6] was performed to obtain the visually distinct areas from the difference image.

The Frequency Spectrum of the difference image (DI) is generated by finding its Fourier transform. The frequency-domain image is split into its amplitude and phase domains. The amplitude-part of the transformed image is then smoothed using a low pass Gaussian kernel. The optimal Kernel size for the Gaussian filter was found to be 0.05 times the image size[3]. This smoothed amplitude allows us to obtain salient regions and remove high-frequency noise. The smoothed amplitude is then recombined with the phase part, and Inverse Fourier transform is used to obtain the time domain image. This Image is then squared and then again passed through a low pass filter of the same kernel size to obtain the final salience map.

This image then undergoes thresholding to give the change candidates for the difference image. If the pixel value is more than the threshold, the pixel value is made to 1. Otherwise, it is made 0. The accuracy of the final result is sensitive to the threshold value t, and consideration must be given to the value of t used. This has been discussed in section 5.3

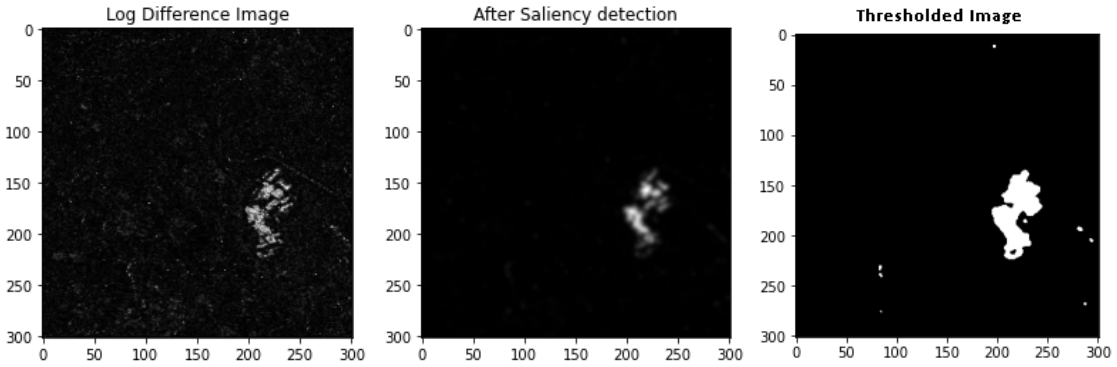

Figure 3: Frequency domain based Saliency detection

4.3 Segmentation using K-means segmentation

The K-means algorithm is used for the segmentation of the difference candidates obtained from the previous step. K is taken to be 3 3, and we divide the change candidate image into 3 segments: Changed area, Unchanged area, and tentative area. Since k-means classifier segments in such a way that the intra-group variance is low and between-group variance is high, we can say that the changed and unchanged segments have high confidence of being in the correct class. The third segment is classified as changed or unchanged by using logistic regression in the next step.

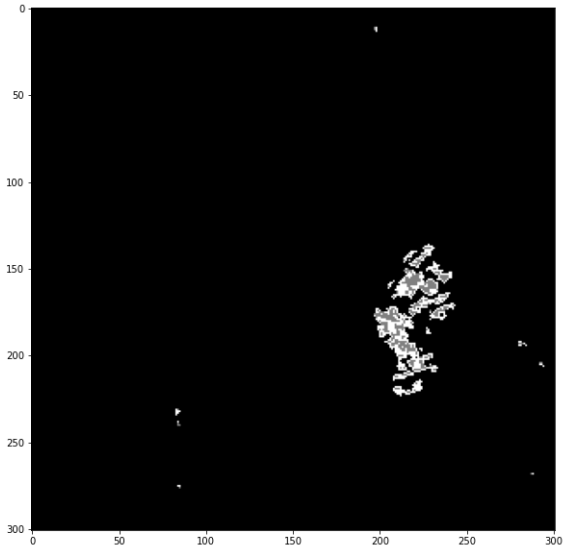

Figure 4: Segmented Change Candidates

4.4 Fine Changed Regions Classification Based on Logistic regression

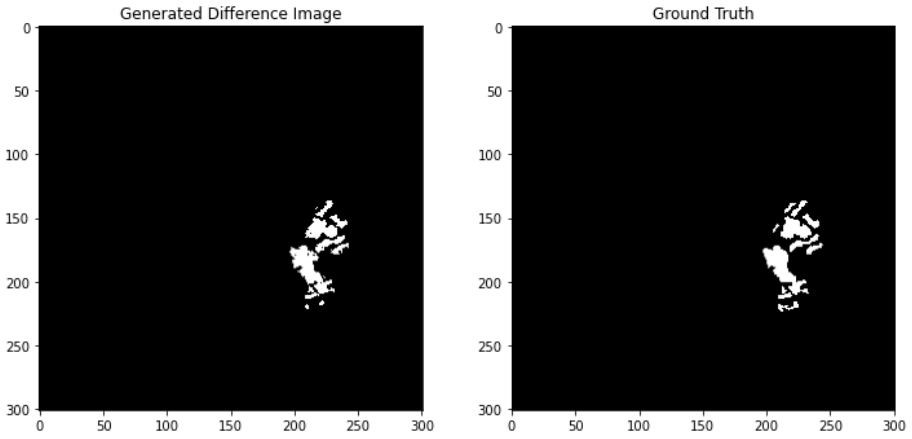

Figure 5: Final Image obtained after Fine region classification

In this step, we use the changed and unchanged segment pixels from the previous step to train a logistic regression model. This model is then used to classify and obtain fine-changed regions from the tentative segment.

Features used for training are obtained by extracting 3 x 3 patches around each pixel from both the multi-temporal images and stacking them to produce a 1 x 18 feature column vector as shown in fig.6. This enables the model to learn the pixel detail and make use of context information and surrounding details.

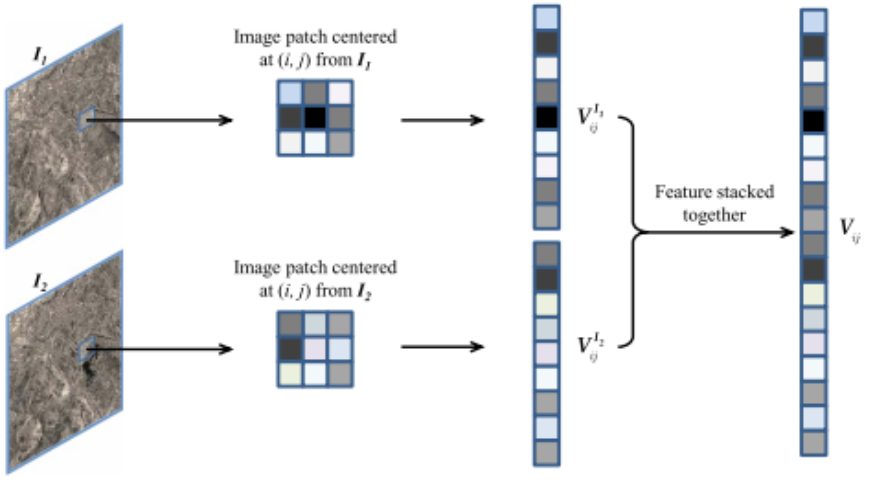

Figure 6: Patch extraction (Ref-[3])

After the classification of the tentative segment, the final difference image is obtained.

5 Test Dataset and Experimental Settings

In order to evaluate the effectiveness of the proposed method, we have applied the proposed method on the Bern-Dataset, Mexico_City_Dataset, Muragia_Dataset, Ottawa_Dataset, and the Yellow River_Dataset. The ground truth change map is crucial for the accuracy assessment of the change detection performance. An inaccurate ground truth change map will lead to improper assessments. Manually annotated ground truth images provided with the dataset were used to evaluate the performance of the algorithm.

5.1 Dataset

The first dataset used in the experiment is the Bern-Dataset, which contains two SAR images obtained from ERS-2 Satellite. The photos were captured in April and May 1999, respectively. The Aare River flooded the areas of Bern entirely between the two dates. In fig.7b, the available ground reality image was provided by the integration of previous data with picture interpretation.

The second dataset utilized in the experiment is Mexico_City_Dataset. As shown in fig.8b, it consists of a section (256×256 pixels) of two SAR images over the city of San Francisco acquired by the ERS-2 SAR sensor. The dataset contains two images obtained in August 2003 and May 2004, respectively.

The following dataset is a section (290×350 pixels) of two SAR images of the city of Ottawa acquired by the RADARSAT SAR sensor. They were provided by Defense Research and Development Canada (DRDC), Ottawa. The picture acquired at the summer floods in May 1997 and the picture obtained in August 1997 at the time of the summer floods are shown in fig.10b. This dataset shows the regions where flooding once occurred. The ground truth image shows the accessible reality provided by the integration of prior knowledge with picture analysis.

The Yellow River dataset shows a representative area of size 257×289 for change detection. The images that were acquired in 2008,2009 and the ground truth change map are shown in fig.11b. It is to be noted that two images are a single-look image and a four-look image. Therefore, the influence of speckle noise in the dataset is much more significant than the other datasets.

Additionally, the Muragia Dataset has also been used for evaluation as shown in fig:9b.

5.2 Evaluation Metrics

Scoring is done based on 3 parameters:

5.2.1 Overall error (OE)

Overall error is calculated as the sum of the total number of miss-classified pixels. This can be represented as the sum of false positives (FP) and false negatives (FN), as shown below.

$$OE = FN + FP$$

5.2.2 Percentage Correct Classification (PCC)

Percentage Correct Classification is the primary metric that has been used to judge the classification efficiency of the model.It gives the number of correctly classified pixels (True positives + True Negatives) as a percentage of the total.

$$PCC = \frac{(TP + TN)}{(TP + TN + FP + FN)} \times 100\%$$

5.2.3 Kappa coefficient (KC)

The Kappa coefficient gives the classification accuracy while taking into consideration the effects of chance (i.e., probability that a random classification is correct) It is defined as

$$KC = \frac{PCC - PRE}{1 - PRE}$$

where PRE is given as

$$PRE = \frac{(TP + FP)(TP + FN)}{(TP + TF + FP + FN)^2} + \frac{(FP + TP)(FP + TN)}{(TP + TF + FP + FN)^2}$$

and stands for the Proportional Reduction in Error.

5.3 Threshold Parameter

The threshold value used in the salience map thresholding significantly affects the final accuracy of the obtained difference image. This value needs to be manually tuned. In general, we observe that a good score can be obtained for threshold values in the 0.05 to 0.2 range.

Thus the difference map generation has been carried out for multiple threshold values in this range, and the best score has been taken as the final score.

6 Experimental Results and Analysis

The difference image was calculated for five datasets given below. All five datasets showed promising results, which can be improved by better tuning the Gaussian kernel size and taking smaller steps while iterating through the threshold values. The generated difference maps have a high degree of correlation to the hand-labeled ground truth and have obtained acceptable scores.

6.1 Bern Dataset

The Bern Dataset showed the best PCC for threshold t = 0.12153846, as seen in fig.7a. The Overall Error (OE) obtained was low, with only 321 miss-classified pixels. The PCC achieved was 99.646. The resultant Kappa coefficient had a value of 85.723.

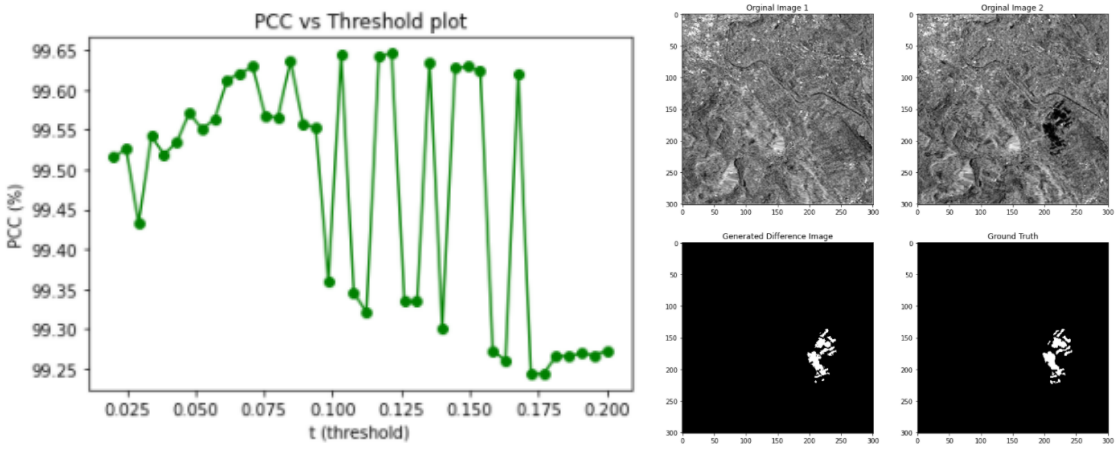

(a) PCC vs threshold

(b) Final Result

Figure 7: Bern Dataset

6.2 Mexico city Dataset

The best PCC was obtained for threshold t = 0.03846154 for the Mexico dataset, as seen in fig.8a. The Overall Error (OE) obtained was 2338, and the PCC achieved was 99.108. The resultant Kappa coefficient had a value of 95.972, which is the highest among all the datasets.

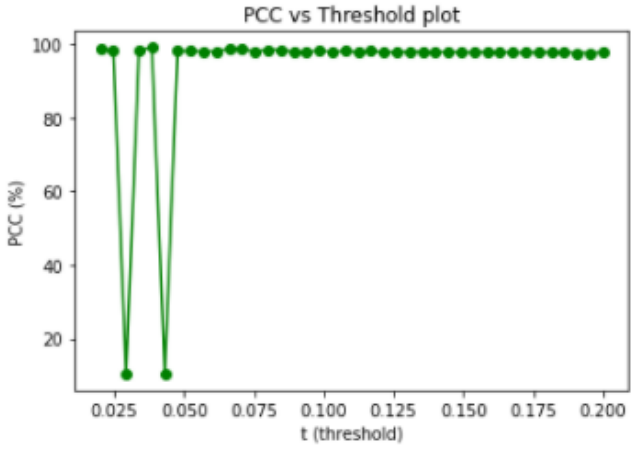

(a) PCC vs threshold

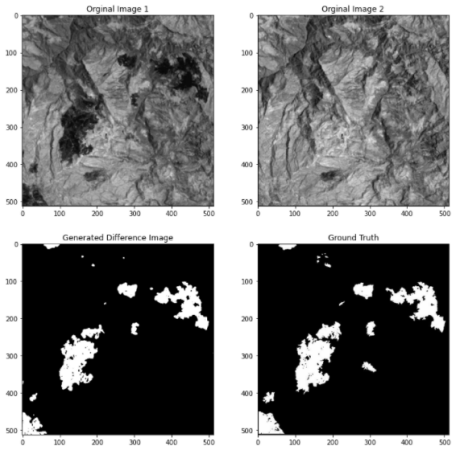

(b) Final Result

Figure 8: Mexico city Dataset

6.3 Muragia Dataset

For the Muragia dataset, the best PCC was obtained for threshold t = 0.18153846, as seen in fig.9a. The Overall Error (OE) obtained was 1880 and the PCC achieved was 98.479. The resultant Kappa coefficient had a value of 86.823.

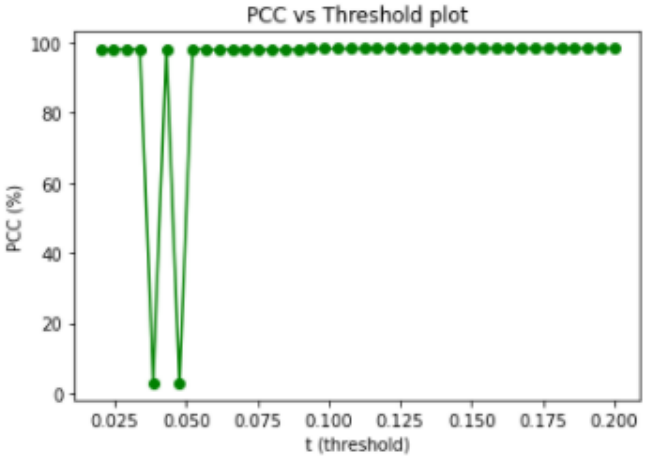

(a) PCC vs threshold

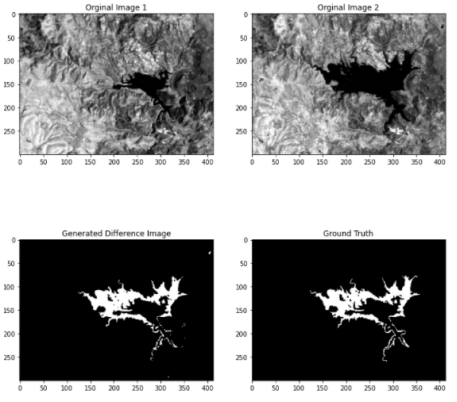

(b) Final Result

Figure 9: Muragia Dataset

6.4 Ottawa Dataset

In the Ottawa dataset, the best PCC was obtained for threshold t = 0.02, as seen in fig.10a. This implies that the performance might be better for even larger threshold values since only values till 0.02 were tested here. The Overall Error (OE) obtained was 3338 for t = 0.02, and the PCC achieved was 96.711. The resultant Kappa coefficient had a value of 86.920.

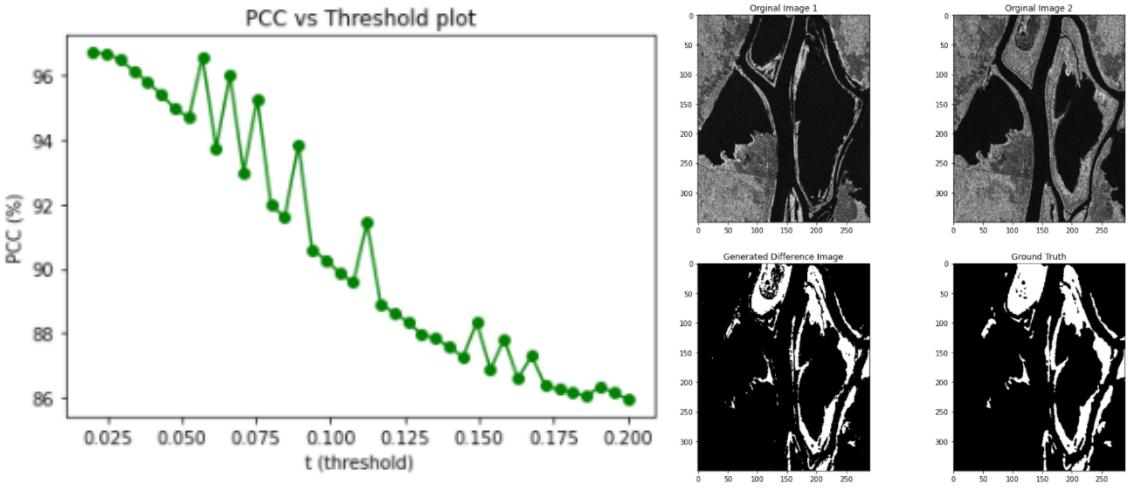

(a) PCC vs threshold **(b)** Final Result

Figure 10: Ottawa Dataset

6.5 Yellow River Dataset

In the Yellow River dataset, the best PCC was obtained for threshold t = 0.05230769, as seen in fig.11a. The Overall Error (OE) obtained was 2873, and the PCC achieved was 96.774. The resultant Kappa coefficient was 61.273.

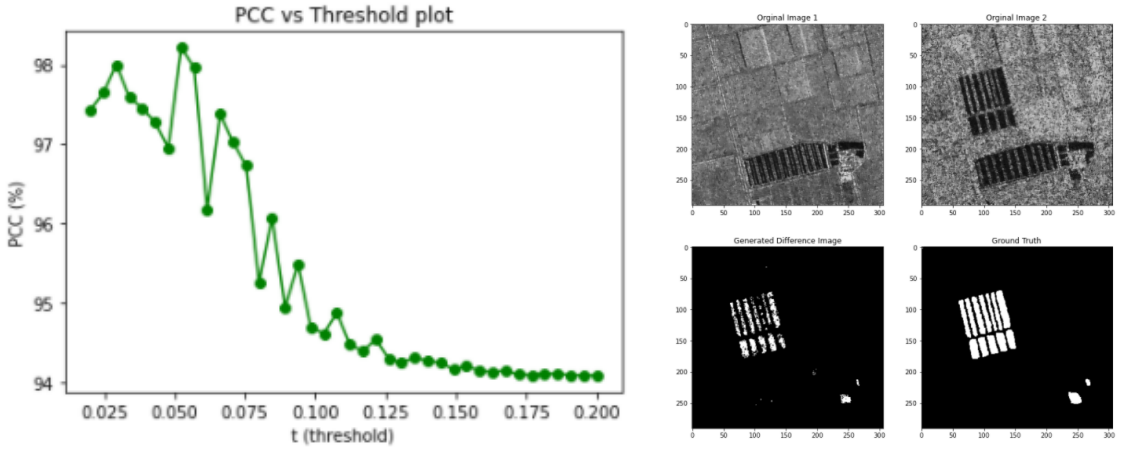

(a) PCC vs threshold

(b) Final Result

Figure 11: Yellow River Dataset

7 Discussion and Conclusion

In this project, a SAR change detection method has been proposed that is based on Frequency domain analysis and logistic regression. In this method, the difference image (DI) is generated by using the log-ratio operator. Frequency domain analysis is performed on the DI to obtain a salience map that on thresholding gives the coarse changed image. This is followed by k-means segmentation, after which the fine-changed regions are obtained using logistic regression to classify the pixels from the middle-tentative segment. The evaluation metrics show that the resultant difference images are very similar to the hand-labeled difference images. Further, it can also be visually observed that the change detection is done correctly and agrees with the two input images. From the experimental results obtained after implementing the proposed algorithm, it can be concluded that the result is effective and that this method can be used for accurate change detection for multi-temporal SAR images.

References

[1] Turgay Celik. "Unsupervised change detection in satellite images using principal component analysis and k-means clustering". In: *IEEE Geoscience and Remote Sensing Letters* 6.4 (2009), pp. 772–776.

[2] Feng Gao et al. "Change detection from synthetic aperture radar images based on neighborhood-based ratio and extreme learning machine". In: *Journal of Applied Remote Sensing* 10.4 (2016), p. 046019.

[3] Feng Gao et al. “Synthetic aperture radar image change detection based on frequency-domain analysis and random multigraphs”. In: *Journal of Applied Remote Sensing* 12.1 (2018), p. 016010.

[4] Maoguo Gong et al. “Fuzzy clustering with a modified MRF energy function for change detection in synthetic aperture radar images”. In: *IEEE Transactions on Fuzzy Systems* 22.1 (2013), pp. 98–109.

[5] Heng-Chao Li et al. “Gabor feature based unsupervised change detection of multitemporal SAR images based on two-level clustering”. In: *IEEE Geoscience and Remote Sensing Letters* 12.12 (2015), pp. 2458–2462.

[6] Jian Li et al. “Visual saliency based on scale-space analysis in the frequency domain”. In: *IEEE transactions on pattern analysis and machine intelligence* 35.4 (2012), pp. 996–1010.